Raman scattering study of the longitudinal optical phonons in ZnSe–ZnS strainedlayer superlattices

Z. P. Guan, X. W. Fan, H. Xia, and S. S. Jiang

Citation: J. Appl. Phys. **78**, 4270 (1995); doi: 10.1063/1.360706
View online: http://dx.doi.org/10.1063/1.360706
View Table of Contents: http://jap.aip.org/resource/1/JAPIAU/v78/i6
Published by the American Institute of Physics.

Raman scattering study of the longitudinal optical phonons in ZnSe–ZnS strained-layer superlattices

Z. P. Guan and X. W. Fan
The Laboratory of Excited State Process, Changchun Institute of Physics, Academia Sinica, Changchun 130021, China

H. Xia and S. S. Jiang
National Laboratory of Solid State Microstructure, Nanjing University, Nanjing 210008, China

(Received 27 October 1994; accepted for publication 14 June 1995)

Raman scattering studies were performed on ZnSe–ZnS strained-layer superlattices with different strains. In the optical phonon regime, the Raman spectra of the ZnSe–ZnS superlattices with a superlattice axis along [001] show optical phonons confined in the ZnSe well and ZnS barrier layers, and display a two-mode behavior corresponding to ZnSe-like and ZnS-like modes. We report the experimental results, by means of Raman scattering of confined longitudinal optical phonons in ZnSe–ZnS strained-layer superlattices. The Raman frequency shift dependence on the layer thickness, superlattice period, and interface strain is presented and discussed. © *1995 American Institute of Physics.*

Raman spectroscopy is a very useful tool to study lattice dynamics in semiconductor low-dimensional structures as well as bulk semiconductors. As is well known, the new periodicity in the growth direction induces folding of the Brillouin zone center of new phonon modes, possibly Raman active. In a multilayer structure, the Raman spectrum will be superposition of the Raman spectra of the individual layers weighed by the scattering probability for phonons of each material. Just like the electrons are mostly confined in one of the materials, the vibration mode of the longitudinal optical phonon (LO) and transverse optical phonon (TO) is confined in the ZnSe and ZnS layers for ZnSe–ZnS strained-layer superlattices (SLS).

Recent results[1–4] with prototype devices based on ZnSe–ZnS, ZnSeS–ZnS, and ZnCdSe–ZnSe superlattices and multiple quantum wells (MQWs) have shown the great potential of this family of materials for device application. Most of the II–VI semiconductor superlattices have a biaxial stress at the heterojunction interface due to the lattice mismatch. Yamamoto *et al.*[5] observed higher order (up to the fifth order) zone-folded acoustic modes in ZnSe–ZnS SLS by means of Raman scattering, and pointed out the Raman spectrum dominantly reflects the periodicity of the superlattices and the roughness of the interface. Reference 6 reported the observation of confined optical modes in the ZnSe layers, interface modes, and additional modes in the frequency range of the vibrations of $ZnSe_{1-x}S_x$. In this paper, we report the first experimental results of confined optical phonons both in the ZnSe well and ZnS barrier layers in ZnSe–ZnS superlattices and calculate the Raman shifts induced by strain.

The superlattice samples in this work were grown on a (100) GaAs substrate by atmospheric pressure metal-organic vapor deposition (MOCVD). Dimethylzinc, dimethylcadmium, and H_2Se are used as the source materials. The substrates were heated at 600 °C under a hydrogen flow prior to growth, in order to eliminate the surface oxide layer. For the $ZnSe_{1-x}S_x$ ($x<0.2$) buffer layer, the growth temperature varied between 280 and 320 °C, and for the ZnS buffer layer the growth temperature was 500 °C. After the growth of the buffer layer the substrate temperature of ZnSe–ZnS SLS were about 400 °C. The structural parameters of the samples used in this paper are listed in Table I.

The Raman measurements were performed in backscattering geometry with the incident photons along the ⟨001⟩ directions and with the incoming and outgoing polarizations lying along the ⟨110⟩ direction. The layer thicknesses of d_{ZnSe} or d_{ZnS} were measured by transmission electron microscopy (TEM) and x-ray diffraction.

Figure 1 shows the x-ray diffraction of ZnSe (0.5 nm)–ZnS (14.5 nm) MQW (QW−1). The full width at half-maximum (FWHM) of 0.15° is observed in this spectrum. Figure 2 shows the first-order Raman spectrum of the above MQW sample (QW−1) with a narrow ZnSe (0.5 nm) well and wide barrier ZnS (14.5 nm) on the $ZnSe_{1-x}S_x$ buffer layer. The peaks labeled LO_1 (269 cm^{-1}) and LO_2 (346.8 cm^{-1}), which are seen in the spectra, can be attributed to the LO phonon modes of ZnSe and ZnS layers induced by the elastic strain. When incident and backscattered light are parallel to the ⟨001⟩ axis, under biaxial stress in the (001) plane the LO and TO modes[7]

$$\Delta\Omega^{LO}=[pS_{12}+q(S_{11}+S_{12})]X/\omega_0^{LO}, \quad (1)$$

$$\Delta\Omega^{TO}=[p(S_{11}+S_{12})+q(S_{11}+3S_{12})]X/(2\omega_0^{TO}), \quad (2)$$

where S_{11} and S_{12} are elastic compliance constants and the strength of stress is

TABLE I. The structure parameters of ZnSe–ZnS SLS.

Sample	Period	Well (nm)	Barrier (nm)	X value
QW−1	100	0.5	14.5	0.92
QW−2	60	2.0	5.0	1
QW−3	40	7.2	3.5	0
QW−4	50	2.0	2.0	0.6

 0021-8979/95/78(6)/4270/3/$6.00

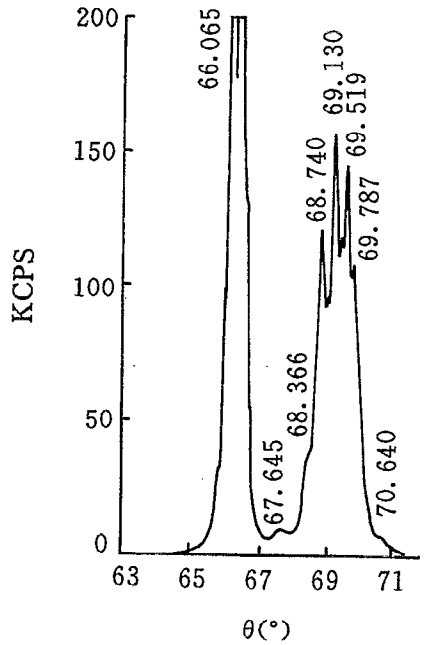

FIG. 1. The X-ray diffraction of ZnSe (0.5 nm)–ZnS (14.5 nm) MQW on the GaAs substrate with the ZnSeS buffer layer.

$$X=\frac{(a''-a_0)}{a_0(S_{11}+S_{12})} \tag{3}$$

and[9]

$$a''=\frac{a_1G_1d_1+a_2G_2d_2}{G_1d_1+G_2d_2}, \tag{4}$$

where G_i are the shear moduli; d_1, d_2 are the layer thicknesses of the ZnSe well and ZnS barrier, respectively. a'' and a_0 are the lattice parameters of SLS parallel to the interface and without strain and a_1, a_2 correspond to ZnSe and ZnS

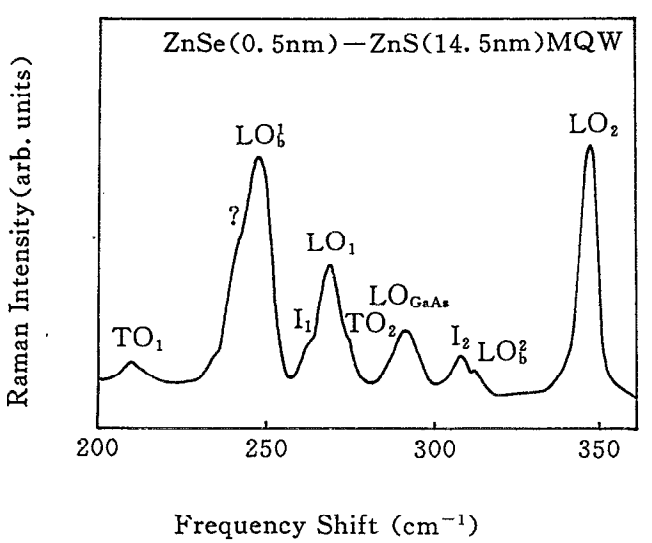

FIG. 2. Raman spectrum of ZnSe (0.5 nm)–ZnS (14.5 nm) MQW with the ZnSeS buffer layer.

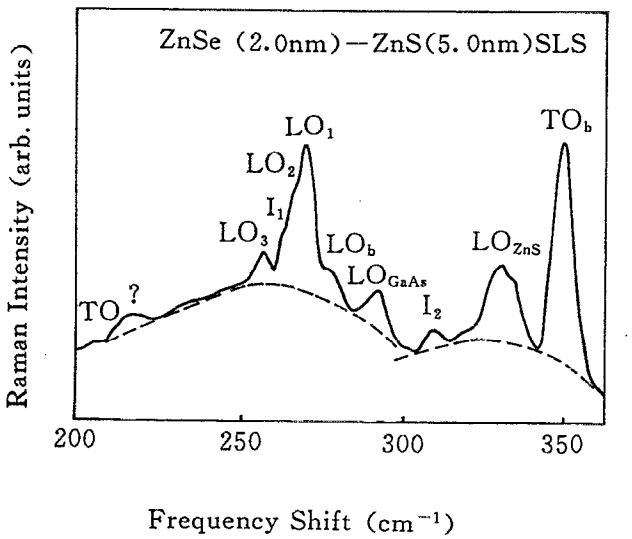

FIG. 3. LO$_m$ modes confined in the ZnSe well layer of ZnSe (2.0 nm)–ZnS (5.0 nm) SLS with the ZnS buffer layer. The bands (dotted line) correspond to the scattering process of the interdiffusion layers between the ZnSe and ZnS interface.

layers. We have used $S_{11}=2.11$ (10^{-12} dyn^{-1} cm^2), $S_{12}=-0.78$ (10^{-12} dyn^{-1} cm^2), $p=-0.41\times10^{28}$, and $q=-0.59\times10^{28}$ for the ZnSe well layer, and $S_{11}=1.89$ (10^{-12} dyn^{-1} cm^2), $S_{12}=-0.72$ (10^{-12} dyn^{-1} cm^2), $p=-0.39\times10^{28}$, and $q=-0.99\times10^{28}$ for the ZnS barrier layer,[8] respectively.

For ZnSe,

$$\Delta\Omega^{LO}=-549.17X(\text{cm}^{-1}), \tag{5a}$$

$$\Delta\Omega^{TO}=-273.85X(\text{cm}^{-1}). \tag{5b}$$

For ZnS,

$$\Delta\Omega^{LO}=-733.07X(\text{cm}^{-1}), \tag{5c}$$

$$\Delta\Omega^{TO}=-177.36X(\text{cm}^{-1}). \tag{5d}$$

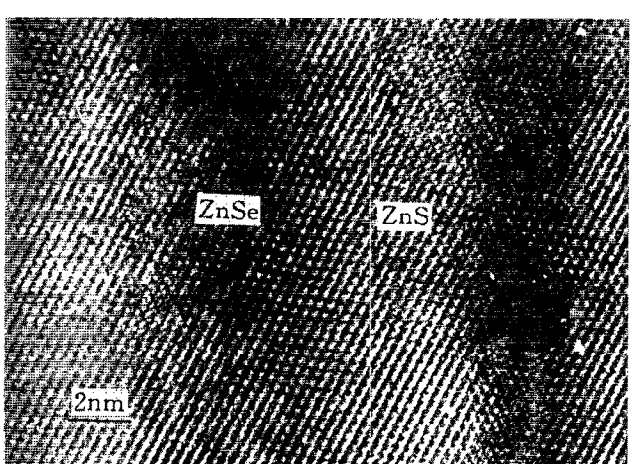

FIG. 4. Uniform interface of ZnSe–ZnS SLS.

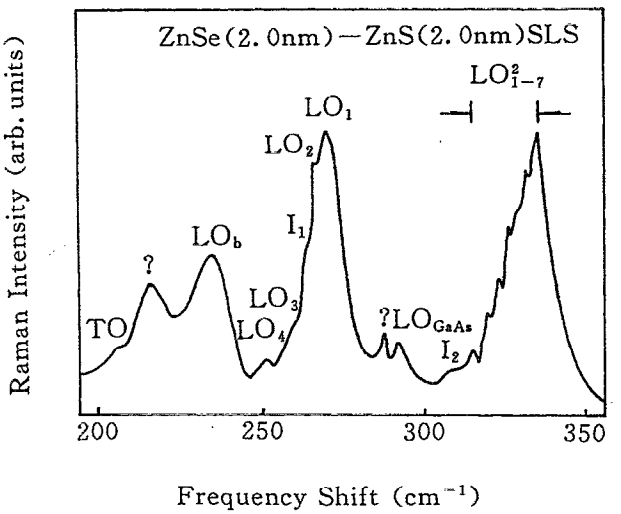

FIG. 5. Two groups of folded LO_m modes both confined in the ZnSe and ZnS layers on ZnSe (2.0 nm)–ZnS (2.0 nm) SLS with the ZnSeS buffer layer. The higher order of LO_m modes in the ZnSe layer are overlaid with the LO_b modes of ZnSeS buffer layers.

In Fig. 2 the frequency shift of ZnSe LO_1, TO_1 phonon modes located at 269 and 208.6 cm^{-1} shift toward the high energies about 17 and 3.6 cm^{-1} in unstrain (LO_{ZnSc}=252 cm^{-1}, TO_{ZnSc}=205 cm^{-1}), respectively. The blue shift of TO mode is less than that of the calculation of Eq. (5b). That result is also observed in other samples. It is noticed that in the more thick ZnS barrier layer (14.5 nm) the LO_2 mode shifts to low energies of about 2.2 cm^{-1}. This value is larger than that of the calculation (0.9 cm^{-1}) with Eq. (5c), which is due to the strain effect between the ZnSeS buffer layer and SLS layers. In Fig. 2 LO^1_b (248 cm^{-1}), LO^2_b (314 cm^{-1}), and LO_{GaAs} (291.5 cm^{-1}) are assigned as the longitudinal optical phonon modes of ZnSe-like, ZnS-like ZnSeS buffer layer and GaAs substrate, and TO_2 (274 cm^{-1}) for the transverse mode of the ZnS layer. In addition, there are other Raman bands marked I_i produced by interface modes, which also appear in other ZnSe–ZnS SLS samples.

The LO confined modes will appear in a narrow range of frequencies because $\omega(q)$ dependence on q has the following relationship:[10]

$$\cos(ka)=1+\frac{\omega^2}{B}\left[\omega^2-\omega(k=0)\right] \tag{6}$$

and[11]

$$k=\frac{m\pi}{(n+1)a}, \quad 1\leqslant m\leqslant n, \tag{7}$$

where a is the common monolayer thickness in ZnSe (0.283 nm) and ZnS (0.270 nm); and n is the number of monolayers; for ZnSe and ZnS B_{ZnSe}=4.5 and B_{ZnS}=8.2×10^8 cm^{-4}, respectively. Figure 3 displays the Raman spectrum of the ZnSe (2.0 nm)–ZnS (5.0 nm) SLS (QW−2) with ZnS buffer layer. Three longitudinal optical (LO_m) lines confined in the ZnSe layer is observed. Under the strain, the LO_{ZnSe} (269.5 cm^{-1}) and LO_{ZnS} (334 cm^{-1}), TO_b (276 cm^{-1}) correspond to the longitudinal and transverse modes of the ZnS buffer layer, and I_1, I_2 are also observed in the same position as well as Fig. 2. It is noticed that there are two bands (dotted line) under the LO_m and LO_{ZnS}. They are attributed to the scattering induced by the interdiffusion layer between ZnSe well and ZnS barrier layers. The higher order confined LO_m modes of the ZnSe layer are overlaid with the above band.

TABLE II. The measured and calculated frequencies (cm^{-1}) of confined LO_m modes in ZnSe and ZnS layers.

m	1	2	3	4	5	6	7
ω_{cal}(ZnSe)	269	266	260.5	253.6	245.1	238	228
ω_{exp}(ZnSe)	269	266	260	253			
m	1	2	3	4	5	6	7
ω_{cal}(ZnS)	335	332	329	325	322	318	315
ω_{exp}(ZnS)	335	332	329	326	322.9	319	315.5

In Fig. 4 it is observed that high-quality ZnSe–ZnS SLS structures (QW−3) without any mismatch defect and dislocation were also obtained. From this high-resolution transmission electron microscopy (HRTEM) image, the interface images are indistinct. This means that there is interdiffusion between ZnSe and ZnS layers grown by MOCVD. Figure 5 shows Raman spectrum of another sample, i.e., ZnSe (2.0 nm)–ZnS (2.0 nm) SLS (QW−4) with ZnSeS buffer layers. In this figure, two groups of the LO_m modes confined in ZnSe and ZnS layers are observed, respectively. Table II lists the calculated and measured frequencies of the LO_m modes in the ZnSe layer and ZnS layer. In the region at about 291–335 cm^{-1}, all of the LO^2_m(m=1–7) modes for the ZnS barrier layer are observed due to no other stronger scattering peak in this region. And for the LO^1_m modes of the ZnSe well layer the higher order (m>4) modes are overlaid with the LO_b (235 cm^{-1}) mode of the ZnSeS buffer layer. In Figs. 3 and 5 other vibration processes labeled "?" are needed for further research.

We have observed the longitudinal optical phonon modes LO_m both in ZnSe well and ZnS barrier layers on ZnSe–ZnS SLS for the first time. We also analyzed the strain properties of ZnSe–ZnS SLS with a different buffer layer. In some samples, the scattering process of interdiffusion layers are discussed.

This work was supported by the High Technology Research Programs in China and the Great National Natural Science Foundation of China.

[1] M. A. Haase, J. Qiu, J. M. Depuydt, and H. Cheng, Appl. Phys. Lett. **59**, 1272 (1991).
[2] H. Jeon, J. Ding, A. V. Nurmikko, H. Luo, N. Samarth, and J. Furdyna, Appl. Phys. Lett. **59**, 1293 (1991).
[3] G. Sun, K. Shahzad, J. M. Gaines, and J. B. Khurgin, Appl. Phys. Lett. **59**, 310 (1991).
[4] H. Jeon, J. Ding, and A. V. Nurmikko, Appl. Phys. Lett. **60**, 2045 (1992).
[5] A. Yamamoto, Y. Kanemitsu, and Y. Masumoto, Appl. Phys. Lett. **61**, 1700 (1992).
[6] D. J. Olego, K. Shahzad, D. A. Cammack, and H. Cornelissen, Phys. Rev. B **88**, 5554 (1988).
[7] A. Yamamoto, Y. Kanemitsu, and Y. Masumoto, Appl. Phys. Lett. **58**, 2135 (1991).
[8] A. Yamamoto, Y. Kanemitsu, and Y. Masumoto, J. Cryst. Growth **117**, 488 (1992).
[9] C. G. Van de walle and R. M. Martin, Phys. Rev. B **84**, 5621 (1986).
[10] B. Jusserand and D. Paquet, Phys. Rev. B **30**, 6245 (1984).
[11] A. K. Sood, J. Menendez, M. Cardona, and K. Ploog, Phys. Rev. Lett. **54**, 2111 (1985).